International Journal of Pharmaceutics 405 (2011) 181–187

Contents lists available at ScienceDirect

International Journal of Pharmaceutics

journal homepage: www.elsevier.com/locate/ijpharm

Pharmaceutical Nanotechnology

Magnetoliposomes prepared by reverse-phase followed by sequential extrusion: Characterization and possibilities in the treatment of inflammation

Sonia García-Jimeno[a], Elvira Escribano[b], Josep Queralt[c], Joan Estelrich[a,*]

[a] Departament de Fisicoquímica, Facultat de Farmàcia, Universitat de Barcelona, Avda. Joan XXIII, 08028 Barcelona, Catalonia, Spain
[b] Departament de Farmàcia i Tecnologia Farmacèutica, Facultat de Farmàcia, Universitat de Barcelona, Avda. Joan XXIII, 08028 Barcelona, Catalonia, Spain
[c] Departament de Fisiologia, Facultat de Farmàcia, Universitat de Barcelona, Avda. Joan XXIII, 08028 Barcelona, Catalonia, Spain

ARTICLE INFO

Article history:
Received 16 September 2010
Received in revised form
17 November 2010
Accepted 24 November 2010
Available online 1 December 2010

Keywords:
Biomaterials
Inflammation
Liposomes
Magnetic properties
Magnetic materials

ABSTRACT

Anionic ferrofluid was encapsulated in 200 nm-diameter liposomes. The process involved phase-reverse evaporation followed by sequential extrusion. Magnetoliposomes were characterized by transmission electron microscopy, Doppler laser electrophoresis, SQUID magnetometry, dynamic light scattering and iron content by atomic absorption spectrophotometry. The absence of hysteresis of the magnetic power of particles at room temperature is characteristic of a material with superparamagnetic properties. The encapsulation efficiency was determined for several iron/phospholipid ratios, and this parameter ranged from 0.016 to 0.024 mg iron per mmole of phospholipids, depending on the initial magnetite concentration. In comparison with magnetoliposomes that were obtained solely by extrusion, this method afforded significantly better encapsulation ($P = 0.0002$). Magnetic particles were intravenously administered to healthy or inflammation-induced mice. After 1 h, the content of iron was determined in exudates, liver, spleen and plasma. Magnetoliposomes accumulated in the exudates collected from the inflammation site, which suggests that these particles could be loaded with the drugs needed to treat some inflammatory processes.

1. Introduction

Nanoparticles offer exciting opportunities for technologies at the interfaces between chemistry, physics and biology, as they form a bridge between bulk materials and atomic or molecular structures. A bulk material should have constant physical properties regardless of its size, but this is often not the case at nanoscale. For bulk materials larger than a few μm, the percentage of atoms at the surface is rather insignificant relative to the total number of atoms of material. However, when the size of the material approaches the nanoscale, the percentage of atoms at the surface becomes significant. Magnetic nanoparticles show considerable promise for a wide range of applications, provided the monodispersity of nanoparticles and the surface properties are controlled (Craig, 1995). The use of magnetic nanoparticles as non-volatile data storage media offers certain advantages over other forms of storage. Moreover, magnetic nanoparticles are or may soon be used in several biomedical applications. For example, the combination of biomolecules with a single magnetic nanoparticle is expected to open new avenues in medical diagnostics, drug targeting or innovative cancer therapies (Reiss and Hütten, 2005; Arruebo et al., 2007). The movements of magnetic nanoparticles can be deliberately controlled and magnetic fields can penetrate human tissues without impediment. Consequently, magnetic nanoparticles can be used to deliver packages, such as anticancer drugs or radionuclide atoms, to a targeted area of the human body. Additionally, magnetic nanoparticles respond strongly to time-modulated magnetic fields, and hence enable dynamic methods of cancer treatment. Alternatively, they could be used to enhance the contrast in magnetic resonance imaging. The ability of such particles to convert magnetic energy into heat by relaxation and hysteresis effects has also gained much attention in antitumor therapy. This simple physical effect could be used to destroy cells directly or to induce a modest rise in temperature that could increase the efficacy of chemotherapy or radiotherapy (Schmitt, 2007). Finally, the viscoelastic architecture inside living cells can be studied by controlled positioning of magnetic nanoparticles inside the internal skeleton of cells. The response of such particles to dynamic magnetic fields can then be followed.

For most of these applications, magnetic nanoparticles are formed by ferromagnetic material such as cobalt, iron or nickel, and particularly by ferrimagnetic iron oxides (maghemite, γ-Fe_2O_3, and magnetite, Fe_3O_4). The magnetic material presents different properties according to particle size. Macroscopic materials (of the order of one micron or more) tend towards the formation of magnetic domains that are characterized by the parallel alignment of magnetic moments on the atomic scale within the

* Corresponding author. Tel.: +34 934024559; fax: +34 934035987.
E-mail address: joanestelrich@ub.edu (J. Estelrich).

0378-5173/$ – see front matter © 2010 Elsevier B.V. All rights reserved.
doi:10.1016/j.ijpharm.2010.11.044

domain, and the relative arrangement of the domains in such a way that the net outer magnetization in the absence of outer fields is minimized. However, in the nanometer range, the formation of magnetic domains is not favoured energetically, and the particles form a single domain, that is, every spin in the particle has the same direction. Hence, the total magnetic moment of the particle is the sum of all spins. The critical diameter for single domain formation is approximately 150 nm for magnetite (Leslie-Peleckie and Rieke, 1996). Data storage media and biomedical sensor systems require a single domain. Particles with this property are called thermally blocked particles. They have long magnetic relaxation times in comparison with the typical time scale of measurements used to study the system. If these nanoparticles are placed in a solid matrix, they exhibit both remanence and coercivity. Medical applications require superparamagnetism at room temperature. This property is displayed in small single domain particles (of the order of tens of nanometers or less, 10–15 nm for magnetite). This phenomenon arises from finite size and surface effects, which dominate the magnetic behaviour of individual nanoparticles. Superparamagnetic particles have fast relaxation times and, consequently, show neither remanence nor coercivity. Thus, these nanoparticles are non-magnetic in the absence of an external magnetic field, but they do develop a mean magnetic moment in an external magnetic field. The advantages of superparamagnetic particles are easy suspension, a large surface area, slow sedimentation and a uniform distribution of the particles in the suspension media (Pankhurst et al., 2003). In biology and medicine, superparamagnetic oxide nanoparticles have been used for cell selection and as magnetic resonance imaging (MRI) contrast agents (Mailänder and Landfester, 2009).

While thermal energy efficiently prevents particles of about 10 nm from sedimentation in a gravitational field or from agglomeration due to magnetic dipole interaction, it does not prevent coagulation due to van der Waals attraction (Odenbach, 2003). To overcome this problem, a protective shell must be created for each particle. This can be achieved using two basic approaches to colloidal stabilization: electrostatic stabilization and/or steric stabilization. In general, nanoparticles are coated with surfactants, polymers, or derivatized lipids. The small size of the stabilized particles results in dispersions, known as ferrofluids, which remain suspended indefinitely in gravitational and moderate magnetic fields (Rosenweig, 1985; Blums et al., 1997).

As demonstrated some decades ago, liposomes comprise colloidal structures which are easy to synthesize, biocompatible and nontoxic (Barenholz, 2001). They can be rendered magnetic by encapsulating magnetic nanoparticles to develop a new type of liposomes known as magnetoliposomes (Bulte and De Cuyper, 2003). Magnetoliposomes can be prepared by trapping the material inside the liposomal aqueous interior during membrane formation by extrusion (Martina et al., 2005; Sabaté et al., 2008; Plassat et al., 2007; Laurent et al., 2008), reverse-phase evaporation (Wijaya and Hamad-Schifferli, 2007), or sonication (Dandamundi and Campbell, 2007) methods, or by means of a completely different strategy. In the latter case, the nanoparticles are stabilized by a surfactant coat. Then, the surfactant molecules are exchanged for phospholipid molecules (De Cuyper and Joniau, 1988; De Cuyper et al., 2003, 2006).

In this study, we encapsulated an anionic ferrofluid in magnetoliposomes by means of a double technique: first, the liposomes were prepared by reverse-phase evaporation using a suspension of ferrofluid as the aqueous medium. Then, the resulting liposomes were extruded through 200-nm pore membranes. After purification, a physicochemical characterization was performed, which included transmission electron microscopy, magnetization analysis, size distribution and encapsulation efficiency. Subsequently, the nanoparticles were tested in mice, with or without an induced inflammatory focus on their back, to follow their biodistribution.

2. Materials and methods

2.1. Materials

Soybean phosphatidylcholine, a zwitterionic phospholipid, (Lipoid S-100) (PC) was donated by Lipoid (Ludwigshafen, EU). Nanoparticles of magnetite stabilized with anionic coating (EMG 707) were purchased from FerroTec (Bedford, NH, USA). The particles had a nominal diameter of 10 nm that was determined by transmission electron microscopy (TEM), a coefficient of viscosity of less than 5 mPa s at 27 °C, and a 1.8% volume content in magnetite. A strong neodymium–iron–boron ($Nd_2Fe_{12}B$) magnet (1.2 T) was obtained from Halde GAC (Barcelona, EU). Reagents were of analytical grade.

2.2. Preparation of magnetoliposomes

Magnetoliposomes were obtained using a modified version of the phase-reverse method (Szoka and Papahadjopoulos, 1978). Phospholipids (100 μmol) dissolved in chloroform/methanol (2:1, v/v) were placed in a round-bottom flask and dried in a rotary evaporator under reduced pressure at 40 °C to form a thin film on the inner surface of the flask. The film was hydrated with 9 mL of diethyl ether and 3 mL of FerroTec suspended in saline solution (0.16 mol L^{-1} NaCl) (diluted from 25% to 1% of the original suspension). The mixture was sonicated for 5 min in a bath sonicator (Transsonic Digital Bath sonifier, Elma, EU) at 0 °C. Once the emulsion had been formed, it was placed in a round-bottom flask and the organic solution was removed at −420–440 mmHg at room temperature. The emulsion became a gel and, finally, this gel transformed into a suspension of liposomes. Once this had been obtained, one mL of saline solution was added and the suspension was rotated at −760 mmHg to remove the ether. Liposomes were diluted with saline solution until a final phospholipid concentration of 20 mmol L^{-1} was obtained. They were then extruded at room temperature into a Liposofast device (Avestin, Canada) through two polycarbonate membrane filters of 0.2 μm pore size a minimum of 9 times both ways (MacDonald et al., 1991).

2.3. Characterization of magnetic particles

The morphology of magnetoliposomes was observed by TEM using a Jeol 1010 microscope (Jeol, Japan) operating at 80,000 kV. Previous to the preparation of the samples, magnetoliposomes were separated from empty liposomes by means of a MACS separation column (Miltenyi Biotech, Bergisch Gladbach, EU). Samples were prepared by placing a drop of the particle suspension onto a 400-mesh copper grid coated with carbon film (in some preparations, the magnetoliposomes were stained with uranyl acetate), and they were allowed to air dry before being inserted into the microscope. Images were recorded with a Megaview III camera. The acquisition was accomplished with Soft-Imaging software (SIS, EU). The iron content of magnetic particles was determined by atomic absorption spectrophotometry in a UNICAM PU 939 flame absorption spectrometer equipped with an acetylene/air (1:1) burner and a selenium hollow cathode lamp (Hereaus), which was operated at 248.3 nm with a 0.5 nm band pass. A reference iron solution (50 μg mL^{-1}) was prepared by dilution of a 1000 μg mL^{-1} solution (Merck, Titrisol, Darmstadt, EU) with double distilled water containing 1% of nitric acid. The measurement of iron was highly linear ($R^2 > 0.997$) over the concentration range of 0.3–3.0 μg mL^{-1}. The reproducibility of the assay was determined by repeated measurements of the reference solution as part of a run or from run to

run. The value (93 ± 2 mg Fe^{3+} per mL of ferrofluid) was the average of three replicates. In the case of magnetoliposomes, iron was measured by atomic absorption spectrophotometry as previously described, and by a colorimetric method based on the titration of ferrous ion by *o*-phenanthroline (Kiwada et al., 1986). Both results coincided. The magnetization of magnetoliposomes and ferrofluid was measured as a function of the applied external magnetic field in a SQUID Quantum Design MPMS XL magnetometer. The external magnetic field was swept from +5000 to −5000 Oe, and then back to +5000 Oe. Measurements were taken at room temperature. The hydrodynamic diameter of magnetoliposomes was determined by dynamic light scattering at 90° with a Zetasizer Nano (Malvern, EU) at 25 °C. The particle size distribution was designated by the polydispersity index (PI), which ranged from 0.0 for an entirely monodisperse sample to 1.0 for a polydisperse sample. The ζ-potential measurements of magnetoliposomes were performed at 25 °C using a Zetasizer Nano ZS (Malvern, EU).

2.4. Encapsulation efficiency determination

To establish the best magnetite/phospholipid ratio, we prepared liposomes hydrated with 1.28–32.11 mg of magnetite per mL of suspension. Non-entrapped ferrofluid particles were removed by size exclusion chromatography (SEC) on Sepharose 4B (GE Healthcare, EU). A total of 250 μL of magnetoliposomes were applied to a 1×30 cm column saturated with lipids before sample elution and eluted with bidistilled water. The amount of encapsulated magnetite was determined on the basis of the ferrous ion using *o*-phenanthroline (Kiwada et al., 1986). The phospholipid content was determined by the Steward-Marshall method (Steward-Marshall, 1980). At high magnetite concentrations, the colour of the ferrofluid is added to the colour developed in the chemical reaction. Consequently, the magnetite must be separated from the phospholipids prior to the phospholipid determination. For this purpose, a MACS separation column was used. If a powerful magnet is placed in the system, iron oxide particles pass through the liposomal membrane. Once it has been verified that phospholipid is recovered at 100% in the effluent, the percentage of encapsulation can be calculated from the magnetite/phospholipid ratio.

2.5. Animal and biological methods

We used twenty-seven eight-week-old female CD-1 mice with a body weight of 28–32 g (Harlam Ibérica, Sant Feliu de Codines, Barcelona, EU). The study was conducted under a protocol approved by the Animal Experimentation Ethics Committee of the University of Barcelona.

The mice were randomly divided into four groups (five animals per group): (a) healthy control-saline (*C*): animals with a back air pouch that received saline intravenously (i.v.) (0.1 mL/10 g body weight); (b) healthy control-magnetoliposomes (*CM*): animals with a back air pouch that received magnetoliposomes i.v. (10 mg of iron/kg body weight); (c) an inflammation-control group (*I*): animals with carrageenan-induced inflammation in the air pouch; and (d) inflammation-magnetoliposomes (*IM*): animals with carrageenan-induced inflammation in the air pouch that received magnetoliposomes i.v. (10 mg of iron/kg body weight).

The method used to induce acute inflammation is similar to that described by Romano et al. (1997). Briefly, sterile air pouches were produced by injecting 5 mL of air subcutaneously into the back of the mouse. Then, 1 mL of sterile saline (groups C and CM) or 1 mL of the phlogogen, 1.2% carrageenan lambda (Sigma–Aldrich, Saint Louis, MO) in saline (groups I and IM), was injected into the air pouch. Five hours later, saline (groups C and I) or magnetoliposomes in saline (groups CM and IM) was administered through the jugular vein to anesthetized (isoflurane, Dr Esteve S.A., Barcelona, EU) mice. The mice were sacrificed twenty min after the saline or magnetoliposome administration.

The iron content in plasma, exudates (pouch) and organs were analyzed by inductively coupled plasma atomic emission spectroscopy (ICP-AES, Perkin-Elmer Optima 3200RL, Massachusetts, USA) after acid digestion of the organic material. The statistical significance of iron concentrations was analyzed using ANOVA. Statistical significance was accepted at the 5% level ($P \leq 0.05$). Values are expressed as mean ± SEM.

3. Results and discussion

3.1. Characterization of magnetic particles

A TEM micrograph of magnetoliposomes is shown in Fig. 1. The size of the magnetoliposomes ranged from 130 to 180 nm and they were full of clusters of particles of ferrofluid. The magnetization curve of the magnetoliposomes is shown in Fig. 2. The saturation magnetization (taken as magnetization at the maximum field of 5 kOe, that is, 0.025 emu g^{-1} or 0.028 emu cm^{-3}; the volume magnetization was calculated by assuming that the density of the overall solution was 1.1 g cm^{-3}) was lower than the theoretical value for the bulk Fe_3O_4 of 96.43 emu g^{-1} (4), but was nevertheless consistent with a magnetic colloid in water (1.8 vol% Fe_3O_4, according to the technical information on the ferrofluid) and encapsulated in liposomes. The magnetization curve also showed negligible remnant magnetization at zero field, which is also characteristic of a soft ferromagnetic material of small dimensions such as magnetite. However, the absence of hysteresis at room temperature demonstrated the superparamagnetic behaviour of the magnetite powder of the magnetic particles.

The dependence of the ζ-potential on pH was investigated in magnetoliposomes. Buffer solutions of pH ranging from 2.25 to 11.30 were prepared with phosphate, citrate and borate solutions. Samples were prepared by adding 1.5 μL of magnetoliposomes to aliquots of 3 mL of each pH solution. The ζ-potential results are shown in Fig. 3. The external phospholipid monolayer conferred a negative charge to the magnetoliposomes for the 3.9–11.30 range of pH, as evidenced by the negative values of ζ-potential determined. At pH 7.4, a ζ-potential value of −26.3 mV was obtained (the pH of

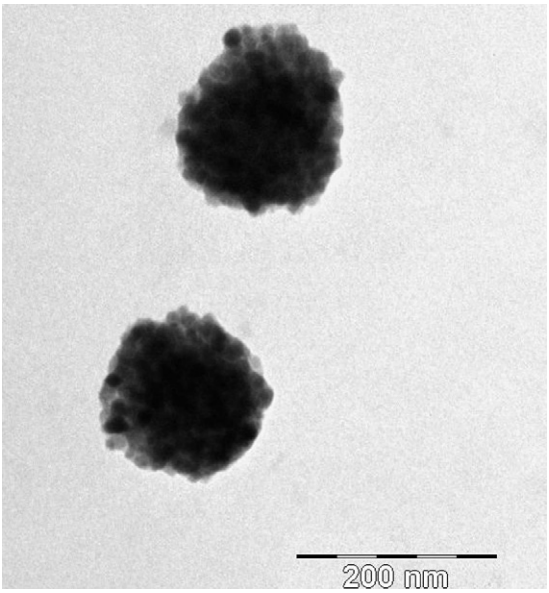

Fig. 1. TEM micrograph of magnetoliposomes. In this figure, the magnetoliposomes were not stained.

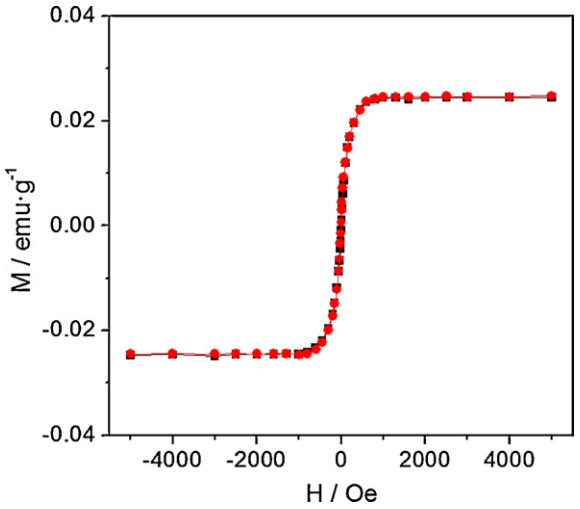

Fig. 2. Mass magnetization as a function of the external magnetic field for magnetoliposomes at ~300 K. The external magnetic fluid was swept from +5000 to −5000 Oe (circles) and then back to +5000 Oe (squares).

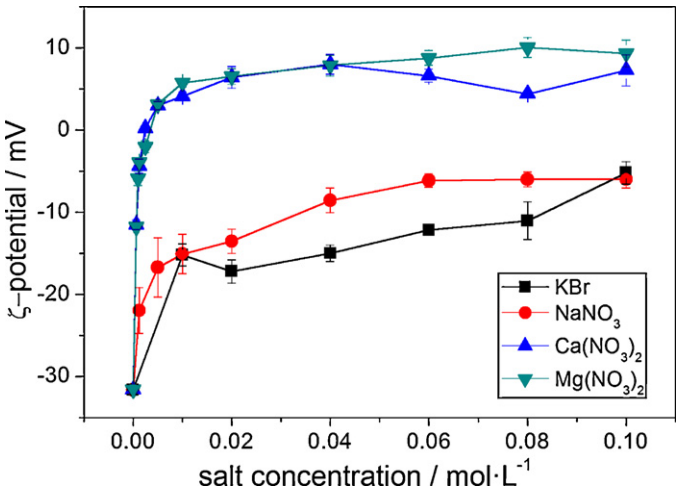

Fig. 4. Influence of electrolytes (monovalent and divalent ions) on electrophoretic properties of magnetoliposomes ($n = 3$).

the saline suspension of magnetoliposomes is 6.7). Under the same conditions, the ferrofluid gave a maximal value of −41.8 mV at a pH of 3.5. Electrostatic stabilization was confirmed by the fact that no sedimentation was observed when magnetoliposomes at pH 7.4 were centrifuged at ~50,000 × *g* for 15 min at room temperature.

The influence of salts on ζ-potential was also checked in magnetoliposomes. In water, magnetoliposomes presented a ζ-potential of −33.2 mV. When a 1:1 electrolyte was added (KBr or $NaNO_3$), the ζ-potential was greatly reduced at the lowest salt concentration used (Fig. 4). After this reduction, the values of ζ-potential underwent a slight, but continuous, variation with salt concentration: an increase in salt concentration was concomitant with less negative values of ζ-potential. A different effect was observed with divalent salts ($Ca[NO_3]_2$ or $Mg[NO_3]_2$). These salts reversed the negative initial values of the charge to the positive values. This finding can be explained by the adsorption of the counter ions on the external layer of the phospholipid. Since positive values were observed at salt concentrations of less than 0.01 mol L^{-1}, such divalent ions clearly have high adsorption ability. Whereas monovalent ions do not produce any aggregation on liposomes, divalent ions, namely calcium and magnesium, result in the aggregation of charged liposomes (Roldán-Vargas et al., 2009).

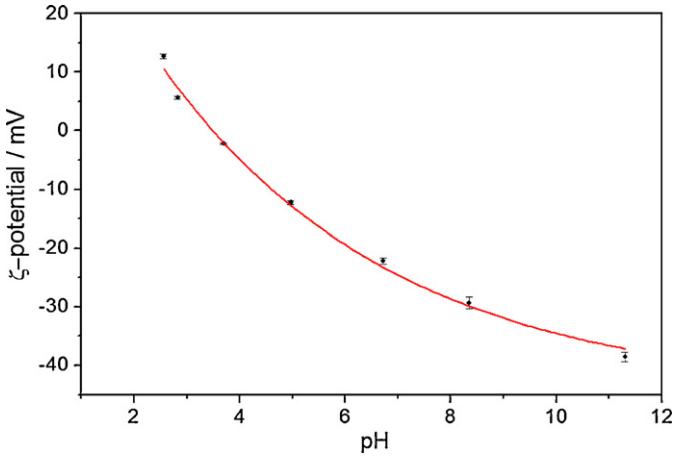

Fig. 3. The ζ-potential of magnetoliposomes as a function of pH. Buffer solutions with an ionic strength of 0.002 were used. Lines are given as a guide ($n = 3$).

Fig. 5 shows the profiles of multilamellar magnetoliposomes and extruded magnetoliposomes before and after the SEC purification of a liposomal sample containing 0.140 g of Fe^{3+} per mmole of phospholipids. The size distribution of ferrofluid is displayed in the inset in Fig. 5. This distribution was centred at 104 nm, and, although monomodal, it was polydisperse (PI = 0.291). The hydrodynamic radius of ferrofluid exceeded the radius of the magnetite particle (10 nm) that was obtained by TEM. Thus, a ferrofluid particle may contain more than one particle of magnetite. The clustering of magnetic nanoparticles has also been observed in magnetite stabilized surfactants (Ditsch et al., 2005; Sabaté et al., 2008). Multilamellar magnetoliposomes obtained after solvent evaporation that did not undergo the extrusion step exhibited a bimodal distribution, with a peak centred at 369 nm (76.2% of the entire intensity) corresponding to magnetoliposomes, whereas the minor peak at 80.5 nm (23.8% of the intensity) corresponded to the non-encapsulated ferrofluid. This pattern was observed for all the iron concentrations tested. After extrusion, a wide, unique peak with maxima between 160 and 190 nm was observed. A value of 187 nm was found for the preparation described above. Purification by size exclusion chromatography afforded a narrower peak with a *z*-mean diameter shifted to approximately 200 nm (in this case, 218 nm). This value is in agreement with the diameter obtained by TEM. These

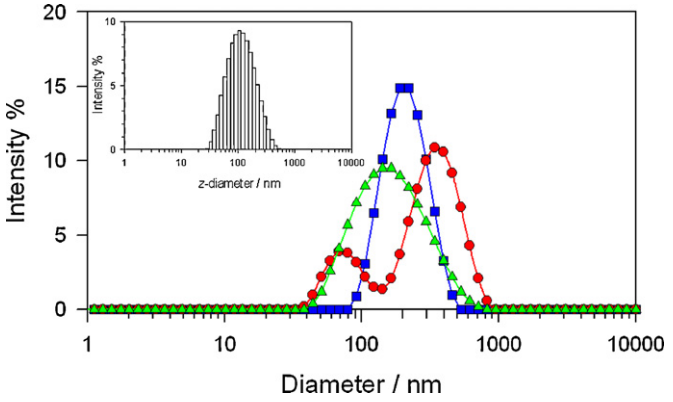

Fig. 5. Distribution of hydrodynamic diameters expressed as *z*-diameters at 298 K of multilamellar magnetoliposomes (red circles), unpurified extruded magnetoliposomes (green triangles), and purified extruded magnetoliposomes (blue squares). The concentration of the samples was 0.140 g Fe^{3+} by mmol of phospholipid. Inset: size distribution of ferrofluid particles. (For interpretation of the references to colour in this figure legend, the reader is referred to the web version of the article.)

Table 1
Encapsulation efficiency of magnetoliposomes.

Initial iron/phospholipid ratio (g/mol) for preparing magnetoliposomes	Final iron/phospholipid ratio (g/mol) for preparing magnetoliposomes after their purification by SEC	Percentage of Fe_3O_4 encapsulated
0.028 + 0.001	0.016 + 0.001	57.1 + 0.1
0.037 + 0.001	0.018 + 0.001	48.6 + 0.1
0.056 + 0.001	0.024 + 0.002	44.6 + 0.1
0.140 + 0.006	0.016 + 0.001	11.4 + 0.1

values imply that the recovered magnetoliposomes were mainly free of contaminating external magnetite, and that the distribution obtained with non-purified magnetoliposomes was the result of overlapping of the ferrofluid and liposome distributions.

3.2. Encapsulation efficiency determination

The encapsulation efficiency was determined in liposomes with varying initial weight/mol ratios of magnetite to phospholipids, ranging from 0.028 g iron/mmol PC to 0.140 g iron/mmol PC. In all set ups, an identical amount of phospholipid was used initially. Magnetite and phospholipid concentrations were determined before extrusion and after purification by chromatography. Table 1 shows the results obtained for encapsulation efficiency.

The amount of encapsulated iron steadily increases as the starting iron/phospholipid ratio increases from 0.028 to 0.056 g iron/mmol PC. The low percentage of encapsulation from 0.140 g iron/mmol PC can be explained by the loss of magnetite during the extrusion process, since the polycarbonate membrane is completely covered by a dark film of magnetite. Although mag-

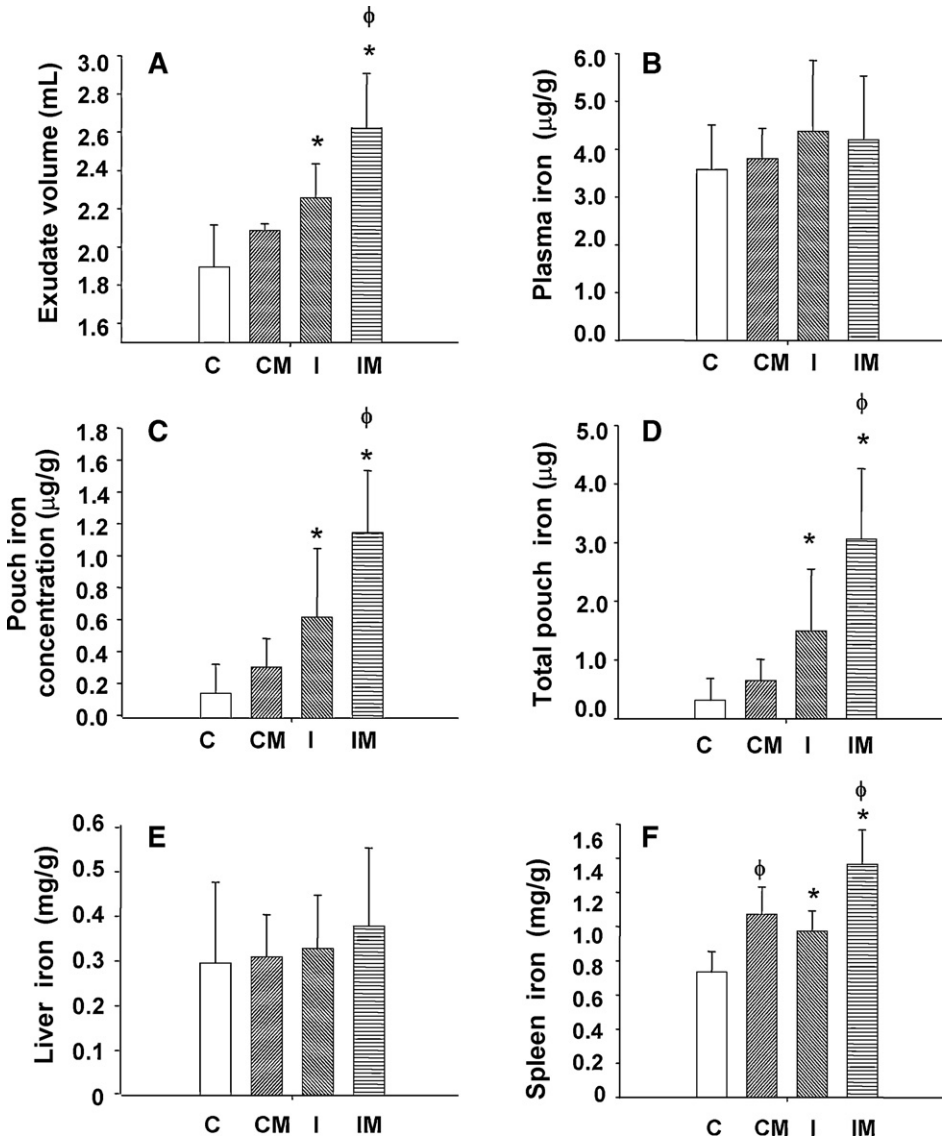

Fig. 6. (A) Pouch volume (mL); (B) plasma iron concentration (μg/mL); (C) pouch (exudates) iron concentration (μg/g); (D) pouch total iron (μg); (E) liver iron concentration (mg/g), and (F) spleen iron concentration (mg/g). Bars represent mean ± SD. From left to right bars correspond to: healthy control mice (C, □), control mice that received magnetoliposomes i.v. (CM, ▨), mice with inflammatory pouch (I, ▧) and mice with inflammatory pouch with magnetoliposomes i.v. (IM, ▤). $P < 0.05$ between control and inflammation groups of mice with or without magnetoliposomes (inflammatory effect). $^{\phi}P < 0.05$ between control and inflammation groups of animals with or without magnetoliposomes (effect of magnetoliposomes).

netite is much smaller than the magnetoliposomes, the formation of clusters of ferrofluid particles could explain the presence of magnetite on the surface of membranes.

As we wanted to determine whether the reverse-phase evaporation presented an improvement in the encapsulation of magnetite, we compared the encapsulation in magnetoliposomes prepared using this method with that obtained by a simple extrusion. In both cases, we used initial ratios of 0.056 g of iron per mmole of phospholipid. After SEC purification, we obtained the following encapsulations: 15.0 ± 1.0 mg iron/mmol PC ($n = 4$) for the extruded magnetoliposomes and 23.8 ± 1.7 mg iron/mmol PC ($n = 4$) for the reverse-phase extruded magnetoliposomes. A statistical analysis of the corresponding means indicated that the encapsulation was significantly different ($P = 0.0002$).

3.3. Biological results

Fig. 6 summarizes the biodistribution of iron after the administration of magnetoliposomes i.v. in mice with or without induced inflammation. Fig. 6A shows the effects of the experimental inflammation on the volume of the exudates. As could be expected, the volume of the pouch exudates in the inflammation control group (I) increased ($P = 0.0255$) in comparison with the healthy control group (C). The volume of exudates in the inflammation-magnetoliposomes group (IM) was also higher than that of the control magnetoliposomes group (CM) ($P = 0.0188$). In the control group, the administration of magnetoliposomes did not increase the volume of exudates. However, an increase in exudate volume was observed in the inflammation group after magnetoliposomes administration ($P = 0.0009$). There was no increase in iron plasma levels (Fig. 6B) after the injection of magnetoliposomes into both healthy and inflammation groups. Plasmas from animals that received magnetoliposomes and those that received saline appeared clear, with no hemolysis.

The iron concentration and total iron in the inflamed air pouch (I) was higher than that of the healthy control non-inflamed air pouch (C) ($P = 0.040$ and $P = 0.056$, respectively) (Fig. 6C and D). This indicates that inflammation produces an increase in iron levels. The same behaviour was observed in animals that received magnetoliposomes: the iron concentration and total iron in the inflamed pouch of animals that received magnetoliposomes (IM) was higher than that of the control animals that received magnetoliposomes (CM) ($P = 0.000$ and $P = 0.003$). In this case, the increase of iron in the inflamed zone (pouch) is a consequence of the inflammation and of the presence of liposomes in this area: the acute inflammatory phase that was produced is characterized by local vasodilatation and enhanced vascular permeability, which facilitates the passage of magnetoliposomes to the inflammatory pouches. As far as the effect of magnetoliposomes on iron levels in the pouch is concerned (Fig. 6C and D), there was no significant increase in iron concentration or total iron in healthy control animals after the administration of magnetoliposomes (C, CM). However, a clear increase in iron concentration and total iron was observed after the administration of magnetoliposomes to animals with air pouch inflammation (I, IM) ($P = 0.018$ and $P = 0.011$).

We did not find any changes that could be attributed to inflammation or magnetoliposomes in the iron concentration in liver (Fig. 6E). However, spleen iron levels increased due to inflammation. Thus, animals with inflammation (with or without magnetoliposomes) had higher iron levels than control animals (without magnetoliposomes [$P = 0.053$] or with them [$P = 0.012$], respectively) (Fig. 6F). After the administration of magnetoliposomes to control animals, the iron levels increased ($P = 0.007$) as they did when magnetoliposomes were administered to animals with inflammation ($P = 0.027$).The levels of basal iron that were found in our study were similar to those reported by Jones et al. (2007). Usually, the highest concentration of magnetic nanoparticles is observed in the liver and spleen (Kim et al., 2006). However in our study, there was no increase in iron concentration in the liver (an organ of the mononuclear phagocytic system) after intravenous administration, whereas there was a clear increase in the spleen compared to the control group (Fig. 6E and F). A similar feature was observed after intraperitoneal administration of magnetic nanoparticles (Kim et al., 2006). Clearly, some factors, such us liposome size, charge and the physical state of the phospholipids used, must determine the specificity of any tissue for magnetoliposomes, and, consequently, for magnetic nanoparticles.

4. Conclusions

Magnetic nanoparticles were encapsulated in liposomes with dimensions of about 200 nm elaborated by reverse-phase evaporation followed by sequential extrusion. The magnetic nanoparticles had superparamagnetic properties. Due to their electrostatic stabilization, we avoided the sedimentation of the magnetic nanoparticles under a gravitational field. Despite the loss of magnetite during the extrusion process, the encapsulation efficiencies achieved with this method were significantly higher than those obtained for magnetoliposomes prepared by simple extrusion.

However, the results of the iron biodistribution study in mice indicate that the magnetic nanoparticles accumulated mainly in the inflammation zone, without the need of a magnet to potentiate the migration of magnetoliposomes to the target site. This suggests that this kind of magnetoliposomes could be used as a system for delivering anti-inflammatory drugs.

Acknowledgment

The authors are grateful for the financial support given by the Spanish Ministerio de Ciencia e Innovación (MICINN) to the project MAT2009-13155-C04-03.

References

Arruebo, M., Fernández-Pacheco, R., Ibarra, M.R., Santamaría, J., 2007. Magnetic nanoparticles for drug delivery. NanoToday 2, 22–32.
Barenholz, Y., 2001. Liposome application: problems and prospects. Curr. Opin. Colloid Interface Sci. 6, 66–77.
Blums, E., Cebers, A., Mairov, M.M., 1997. Magnetic Fluids. Walter de Gruyter, Berlin.
Bulte, J.W.M., De Cuyper, M., 2003. Magnetoliposomes as contrast agents. Methods Enzymol. 373, 175–198.
Craig, D., 1995. Magnetism-Principles and Applications. Wiley, Chichester.
Dandamundi, S., Campbell, R.B., 2007. Development and characterization of magnetic cationic liposomes for targeting tumor microvasculature. Biochim. Biophys. Acta 1768, 427–438.
De Cuyper, M., Joniau, M., 1988. Magnetoliposomes. Formation and structural characterization. Eur. Biophys. J. 15, 311–319.
De Cuyper, M., Müller, P., Lueken, H., Hodenius, M., 2003. Synthesis of magnetic Fe_3O_4 particles covered with a modifiable phospholipids coat. J. Phys.: Condens. Matter. 15, S1425–S1436.
De Cuyper, M., Caluwier, D., Baert, J., Cocquyt, J., Van der Meeren, P., 2006. A successful strategy for the production of cationic magnetoliposomes. Z. Phys. Chem. 220, 133–141.
Ditsch, A., Laibinis, P.E., Wang, D.I.C., Hatton, T.A., 2005. Controlled clustering and enhanced stability of polymer-coated magnetic nanoparticles. Langmuir 21, 6006–6018.
Jones, B.C., Beard, B.L., Gibson, J.N., Unger, E.L., Allen, R.P., McCarthy, K.A., Early, C.J., 2007. Systems genetic analysis of peripheral iron parameters in the mouse. Am. J. Physiol. Regul. Integr. Comp. Physiol. 293, 116–124.
Kim, J.S., Yoon, T.-J., Yu, K.N., Kim, B.G., Park, S.J., Kim, H.W., Lee, K.H., Park, S.B., Lee, J.-K., Cho, M.H., 2006. Toxicity and tissue distribution of magnetic nanoparticles in mice. Toxicol. Sci. 89, 338–347.
Kiwada, H., Sato, J., Yamada, S., Kato, Y., 1986. Feasibility of magnetic liposomes as a targeting device for drugs. Chem. Pharm. Bull. 34, 4253–4258.
Laurent, S., Vander Elst, L., Thirifays, C., Muller, R.N., 2008. Paramagnetic liposomes: inner versus outer membrane relaxivity of DPPC liposomes incorporating gadolinium complexes. Langmuir 241, 4347–4351.
Leslie-Peleckie, D.L., Rieke, R.D., 1996. Magnetic properties of nanostructured materials. Chem. Mater. 8, 1770–1783.

MacDonald, R.C., MacDonald, R.I., Menco, B.P., Takeshita, K., Subbarao, N.K., Hu, L.R., 1991. Small-volume extrusion apparatus for preparation of large, unilamellar vesicles. Biochim. Biophys. Acta 1061, 297–303.
Mailänder, V., Landfester, K., 2009. Interaction of nanoparticles with cells. Biomacromolecules 10, 2379–2400.
Martina, M.S., Fortin, J.P., Ménager, C., Clément, O., Barratt, G., Grabielle-Madelmont, C., Gazeau, F., Cabuil, V., Lesieur, S., 2005. Generation of superparamagnetic liposomes revealed as highly efficient MRI contrast agents in vivo imaging. J. Am. Chem. Soc. 127, 10676–10685.
Odenbach, S., 2003. Ferrofluids – magnetically controlled suspensions. Colloid Surf. A 217, 171–178.
Pankhurst, Q.A., Connolly, J., Jones, S.K., Dobson, J., 2003. Applications of magnetic nanoparticles in biomedicine. J. Phys. D 36, R167–R181.
Plassat, V., Martina, M.S., Barratt, G., Ménager, C., Lesieur, S., 2007. Sterically stabilized superparamagnetic liposomes for MR imaging and cancer therapy: pharmacokinetics and biodistribution. Int. J. Pharm. 344, 118–127.
Reiss, G., Hütten, A., 2005. Magnetic nanoparticles. Applications beyond data storage. Nat. Mater. 4, 725–726.
Roldán-Vargas, S., Barnadas-Rodríguez, R., Quesada-Pérez, M., Estelrich, J., Callejas-Fernández, J., 2009. Surface fractals in liposome aggregation. Phys. Rev. E. 79, 011905-1–011905-14.
Romano, M., Faggioni, R., Sironi, M., Sacco, S., Echtenacher, B., Di Santo, E., Salmona, M., Ghezzi, P., 1997. Carrageenan-induced acute inflammation in the mouse air pouch synovial model. Mediators Inflamm. 6, 32–38.
Rosenweig, R.E., 1985. Ferrohydrodynamics. Cambridge University Press, London.
Sabaté, R., Barnadas-Rodríguez, R., Callejas-Fernández, J., Hidalgo-Álvarez, R., Estelrich, J., 2008. Preparation and characterization of extruded magnetoliposomes. Int. J. Pharm. 347, 156–162.
Schmitt, A.M., 2007. Thermoresponsive magnetic colloids. Colloid Polym. Sci. 285, 953–966.
Steward-Marshall, J.C., 1980. Colorimetric determination of phospholipids with ammonium ferrothiocyanate. Anal. Biochem. 104, 10–14.
Szoka, F., Papahadjopoulos, D., 1978. Procedure for preparation of liposomes with large internal aqueous phase and high capture by reverse-phase evaporation. Proc. Natl. Acad. Sci. U.S.A. 75, 4194–4198.
Wijaya, A., Hamad-Schifferli, K., 2007. High-density encapsulation of Fe_3O_4 nanoparticles in lipid vesicles. Langmuir 23, 9546–9550.